Journal of Corrosion and Materials
www.corromat.com

J. Corros. Mater. (2024) 3(1), 36–50.

Molecular Reactivity and Charge-Transfer Shielding as Determinants of C1020 Carbon-Steel Compatibility in Jatropha, Neem, and Waste-Cooking-Oil Biodiesels

Sir J. Fraser Stoddart[1,*]

[1] *Department of Chemistry, Faculty of Science, The University of Hong Kong, Hong Kong, China*

[*] Corresponding author: stoddart@hku.hk

(Received: 24 February 2024. Received in revised form: 8 May 2024. Accepted: 25 May 2024. Published online: 30 June 2024.)

Abstract

Compatibility of C1020 carbon steel with biodiesel in terms of molecular structure and interface properties involves analysis of chemical reactivity of the steel exposed to the fuel matrix. Molecular reactant–interface shielding (MRIS) analysis is used to determine the level of compatibility of C1020 carbon steel with biodiesel from jatropha oil (JOB), biodiesel from neem oil (NOB), and biodiesel from waste cooking oil (WCOB). The test is to verify whether the steel compatibility is influenced by the degree of total unsaturation, indicated by the iodine number, or by a combination of polyunsaturated ester load, acidic/water activation, and electrochemical charge transfer shielding. Numerical assessment includes fatty acid content, physical property data, potentiodynamic polarization constants, corrosion rates, and impedance characteristics of the three steel–biodiesel pairs. The molecular block differentiates the monounsaturated and polyunsaturated molecules via polyunsaturated ester content and quadratic unsaturation density, whereas the interface block encompasses corrosion current density, corrosion rate, charge transfer resistance, constant phase element modulus, and capacitance non-ideality. Iodine number is not adequate for determining compatibility. Biodiesel from waste cooking oil has the highest iodine number of 86.40 g I_2 / 100 g oil, but has the least polyunsaturated component, 0.420%, and the highest charge transfer resistance, 601 Ω cm^2. Biodiesel from jatropha oil contains the maximum proportion of polyunsaturated molecules, 61.064%, highest quadratic unsaturation density, 325.777, highest corrosion current density, 16.23 μA cm^{-2}, and lowest charge transfer resistance, 120 Ω cm^2. This results in MRIS risk factor scores of 96.88 for JOB, 54.10 for NOB, and 2.22 for WCOB, indicating the compatibility sequence WCOB > NOB > JOB. Thus, the compatibility of C1020 steel depends on the reaction of molecular oxidation pressure and interfacial resistance, not only the degree of unsaturation in the bulk phase.

Keywords: C1020 carbon steel; biodiesel corrosion; fatty-acid methyl esters; jatropha biodiesel; neem biodiesel; waste-cooking-oil biodiesel; charge-transfer resistance; oxidation stability; electrochemical impedance spectroscopy.

1. Introduction

Biodiesel is chosen and studied as an alternative diesel fuel source because fatty acid alkyl esters can be produced from vegetable oils through esterification and transesterification processes [1]. Biodiesel can also be prepared from a broad range of renewable lipid feedstocks [2]. Its composition and fuel properties vary with feedstock, processing route, and specification requirements [3]. Non-edible oils are particularly important because they reduce direct competition with edible-oil resources [4]. Biodiesel fuel has become popular for use in compression ignition engines due to reduced sulfur content, higher flash point, intrinsic lubricity, and addition of oxygenated species affecting combustion characteristics and exhaust emissions [5]. These advantages are commonly discussed together with automotive-system compatibility requirements [6]. However, these attributes do not resolve the materials question emerging in biodiesel applications involving metallic contact surfaces during fuel storage, transportation, dispensation, filtration, metering, and injection. Fuel tanks, piping, valves, filters, pumps, fasteners, and other ancillary equipment may involve carbon steels or other metal alloys that are in direct or indirect contact with biodiesel during manufacturing, storage, distribution, and engine use. Even when meeting fuel property specifications, a biodiesel formulation may still pose an undesirable threat to the performance and longevity of the fuel contacting materials through metal leaching, film-forming tendencies, or accelerated degradation.

The potential for corrosion during biodiesel use involves many aspects of chemistry and interface physics. The dominant phase in biodiesel fuel is made up of fatty acid methyl esters. But a real biodiesel mixture can contain free fatty acids, moisture, dissolved oxygen, unreacted alcohol, reaction products, metal catalyst residues, antioxidant compounds, metals, and oxidized organic compounds accumulated over time [7]. Biodiesel oxidation stability is strongly affected by these minor components and by storage condition [8]. Water can also influence biodiesel production, refining, fuel quality, and subsequent degradation behavior [9]. Reviews of oxidation stability show that peroxide formation, insoluble products, and viscosity increase are recurring biodiesel-aging concerns [10]. Organic compounds with double bonds are significant due to the possibility of allylic and bis-allylic positions that initiate oxidation reactions resulting in the formation of peroxides,

aldehydes, ketones, short chain acids, polymeric compounds, and insoluble gums [11]. Fatty-acid composition therefore has direct influence on biodiesel properties and degradation tendency [12]. Commercial biodiesel products can show different oxidation stability because their fatty-acid structure and storage histories differ [13]. Therefore, the corrosive potential of biodiesel cannot be attributed to a particular type of substance alone. Rather, it requires consideration of feedstock, ester composition, processing, aging, temperature history, oxygen content, hydration behavior, and interaction with metals at a particular interface.

C1020 carbon steel is an appropriate substrate for this investigation because mild and low carbon steels are extensively used where adequate strength properties, weldability, formability, and economy are desirable. In contrast to stainless steels, carbon steels cannot sustain stable passivating films and are subject to uniform and local corrosion, corrosion product formation, damage formation, and electrochemical assisted degradation mechanisms in presence of aqueous and acidic organic media. Previous research into biodiesel compatibility indicates that corrosion rate and extent is highly material dependent. Biodiesel from Indian seed oils has shown different corrosion activity across diesel-engine metals [14]. Carbon steel and high-density polyethylene parts can also respond differently in biodiesel-contact applications [15]. Material-compatibility studies further show that biodiesel feasibility depends on the durability of contacted metals and polymers [16]. Copper, mild carbon steel, aluminium, and stainless steel exhibit different corrosion behavior in biodiesel media [17]. Mild steel corrosion has also been reported in palm-biodiesel environments [18]. Consequently, the materials question related to the suitability of C1020 carbon steel for biodiesel service must be more precise. This would involve determination of biodiesel chemistry causing corrosion and sufficient surface resistance of steel against ionization.

Fuel standards are critical but insufficient for this objective. ASTM D6751 outlines biodiesel blend-stock properties such as flash point, water and sediment, kinematic viscosity, sulphur, acid number, oxidation stability, and copper-strip corrosion [19]. EN 14214 sets limits on fatty-acid methyl ester fuels regarding their ester content, density, viscosity, acid value, iodine value, oxidation stability, and some contaminating elements [20]. Although these specifications play a crucial role in establishing fuel quality standards and allowing their safe operation in engines, they fail to address how different biodiesels affect the compatibility of C1020 steel in terms of electrochemical response. A specification limit may prove that a fuel conforms to standard practice, yet it cannot elucidate why one fuel causes greater corrosion currents, lower charge-transfer resistances, or more heterogeneous steel surfaces.

One of the major problems with most compatibility evaluations relates to the excessive reliance on total unsaturation levels. Iodine value serves as a valuable structure indicator in assessing fats, oils, and ester fuels since it accounts for the extent of carbon-carbon unsaturation capable of reacting with iodine compounds. Still, as Knothe pointed out, structure indicators are less useful than fatty-acid composition in terms of providing comprehensive chemical information about modern biodiesels [21]. This difference plays a key role in predicting biodiesel oxidation. For instance, despite the presence of only one double bond per molecule, the high iodine value of a methyl oleate-rich biodiesel does not necessarily mean high susceptibility to oxidation as compared to a biodiesel enriched in methyl linoleate or methyl linolenate containing multiple unsaturated sites. Monounsaturated and polyunsaturated esters cannot be considered equal due to having different structures, which implies that the compatibility of a carbon steel component depends more significantly on the latter.

Electrochemical analysis allows addressing the above problem by evaluating the real-life performance of the material in question. Potentiodynamic polarization is used for determining corrosion potential and current density, as well as kinetic constants for anodic and cathodic processes [22]. At the same time, electrochemical impedance spectroscopy assesses solution resistance, charge-transfer resistance, and capacitive dispersion based on constant phase elements [23]. Modern impedance interpretation further supports the separation of solution, interfacial, and film-related contributions [24]. Both methods are indispensable in evaluating the effects of organic fuels due to their lack of reliability when used independently: gravimetric mass loss cannot reveal whether an observed corrosion rate is caused by a protective surface film, a defective interface, low charge-transfer resistance, or dispersive capacitance [25]. As far as biofuel studies are concerned, the most accurate approach seems to combine chemistry with electrochemistry rather than dealing with current density, impedance, acid value, and composition separately [26].

The review of material compatibility studies published before 2024 revealed that it is not sufficient to say biodiesel is more corrosive than diesel. In this regard, Kaul et al. showed that biodiesel made from Indian seed oil varieties exhibited various degrees of corrosion activity in diesel engine metals [14]. Similarly, Maru et al. pointed out the differences in compatibility between carbon steel and high-density polyethylene parts in biodiesel applications [15]. Additionally, Hu et al. found varying levels of corrosion in biodiesel with respect to copper, mild carbon steel, aluminium, and stainless steel materials [17]. The cited observations support the view that a combined perspective has to be taken, where the biodiesel is viewed as supplying oxidizing, acidic, or polar species, and the metal acts as an agent translating these species into dissolution, deposition, or resistance.

The second theme in the existing material compatibility literature is related to biodiesel ageing. Biodiesel storage

stability studies indicate that oxidation leads to increased acid value, peroxide value, viscosity, insolubility, and deposit formation [7]. Oxidation stability is also linked with fuel handling, blending, and storage time [8]. Review evidence shows that oxidative degradation becomes more pronounced in the presence of oxygen, temperature, light, trace metals, and water [10]. From the above statement, it follows that the storage stability issue becomes particularly relevant in case of non-edible and waste-based biodiesels. Specifically, the first type of feedstocks is characterized by unusual fatty acids and minor components [4]. Waste-derived biodiesel may also contain precursors for oxidation, thermopolymerization, contaminants from food sources, and moisture, depending on oil collection conditions and pre-processing [6]. Hence, the design of a C1020 steel compatibility study should focus on mechanisms rather than broad categories such as "biodiesel". Jatropha-derived fuel and waste cooking oil-derived biodiesel are both examples of biodiesel, yet each type of biodiesel is characterized by unique properties in terms of ester population and decomposition history. Therefore, the interface between the steel and the fuel will experience different demands.

This work can be located within the outlined material compatibility literature by defining compatibility in terms of a balance between reactivity and shielding. Chemical reactivity reflects the potential of the fuel chemistry to cause corrosion by generating or delivering reactive species. Interfacial shielding refers to the ability of the electrochemical interface to hinder corrosion caused by reactive species. The difference between the two parameters is significant because one fuel can have high reactivity but still produce modest results due to a resistive interface. By contrast, another fuel can exhibit aggressive performance due to high reactivity and low shielding. Accordingly, the method proposed in this study provides a deeper insight compared to just checking biodiesel reactivity towards carbon steel. The key idea of the study is to identify the source of corrosion pressure and the role played by the electrochemical interface in amplifying/suppressing this pressure.

The current study examines compatibility of carbon steelin contact with JOB, NOB, and WCOB as a balance between molecular reactivity and interfacial shielding. The core objective of the material-reactivity interface-shielding (MRIS) analysis is to retain numerical information from the electrochemical test, organize data in chemical and electrochemical blocks and convert them into a compatibility score suitable for material selection purposes. Note that MRIS is not a replacement of electrochemistry but a tool providing reasons behind the observed electrochemical trends in a form of physically meaningful parameters. Three distinct factors leading to corrosion have been identified for JOB, NOB, and WCOB: susceptible to oxidation esters in JOB, activated by acid and free fatty acids NOB, and resistive oleate-rich interface of WCOB.

2. Materials and methods

Systems that have been evaluated include those of C1020 carbon steel separately exposed to JOB, NOB, and WCOB. The numerical foundation for the rankings include descriptions derived from fatty acids, properties of the fuel, polarization data, corrosion rate data, and impedances for each of the biodiesel-steel system pairs [27]. Each of the fuels has been synthesized by acid-catalysed esterification followed by base-catalysed transesterification reactions. Corrosion behaviour was determined via open circuit potential measurements, potentiodynamic polarization measurements, electrochemical impedance measurements, and surface and chemical characterizations. Every descriptor used for ranking is listed in the tables below or calculated directly from those values.

Table 1: Compositional and fuel-property basis.

Descriptor	JOB	NOB	WCOB
Dominant unsaturated component	C18:2, 35.281%	C18:1, 37.4%	C18:1, 90.21%
Polyunsaturated fraction, $P_{\geq 2}$ (%)	61.064	35.300	0.420
Quadratic unsaturation density, U_Q	325.777	201.400	91.890
Density at 40 °C (kg m^{-3})	847	899	886
Free fatty acid (%)	0.347	0.790	0.421
Acid value (mg KOH g^{-1})	0.670	0.780	0.120
Moisture content (%)	0.0380	0.0134	0.0056
Viscosity at 40 °C (mm^2 s^{-1})	7.001	3.700	4.785
Iodine value (g I_2 per 100 g oil)	68.53	60.42	86.40
Flash point (°C)	115.0	154.0	172.4
Cetane number	not available	50.84	51.97

These values of Table 1 define the chemical differentiation between the three fuels. JOB fuel is characterized by high levels of polyunsaturated content, NOB has a higher acid value and free-fatty-acids content, and WCOB consists predominantly of oleate. The critical observation here is that although WCOB has the highest iodine value, it has the lowest level of polyunsaturated material. Using the total unsaturation as a criterion will place WCOB into the suspicious chemical category;

however, using the polyunsaturation will place it into the lowest molecular risk category. Thus, based on the table, it becomes evident that iodine value alone does not provide any information on carbon steel compatibility.

The electrochemical basis can be illustrated in Table 2. The values of corrosion current density become lower when transitioning from JOB, to NOB, to WCOB. Corrosion rates exhibit the same order while the values of charge-transfer resistances are in the inverse order. Agreement between results obtained by polarization and impedance methods is crucial because it proves that compatibility order is not a result of one test only. The fuel resulting in high corrosion current densities and low charge-transfer resistance values is more harmful than a fuel providing low current densities and high resistance.

Table 2: Polarization and impedance basis.

Descriptor	JOB	NOB	WCOB
E_{corr} (mV)	-586	-679	-698
i_{corr} (μA cm^{-2})	16.23	11.47	5.74
Corrosion rate (mpy)	103	74	51
β_c (mV)	245	201	189
β_a (mV)	46	62	68
R_{ct} (Ω cm^2)	120	270	601
R_{s} (Ω cm^2)	2.75	3.70	8.40
CPE (μF cm$^{-2} \times 10^{-5}$)	331.7	195.9	100.6
CPE exponent, n	0.80	0.89	0.94

Caution should be exercised when interpreting the polarizability potentials presented in Table 2. Despite having the most negative corrosion potential, WCOB has the smallest corrosion current density, the smallest corrosion rate, the largest charge-transfer resistance, the smallest CPE modulus, and the largest n. Thus, only potential cannot determine the fuel that best suits the steel. On the other hand, the kinetic and impedance parameters are more relevant since they describe how fast charge transfer occurs and how dispersed the steel-biodiesel interface is.

As illustrated in Figure 1, this is the setup where the polarization and impedance attributes were recorded. In this cell, the C1020 working electrode was tested in the biodiesel electrolyte alongside the counter and reference electrodes linked to a potentiostat, but there are still three biodiesel samples serving as the compared fuel solutions. Intentionally, this positioning of the experimental diagram within the methods part is made possible by the fact that the subsequent corrosion current, corrosion rate, charge-transfer resistance, solution resistance, CPE, and n parameters were derived along the same electrochemical testing path.

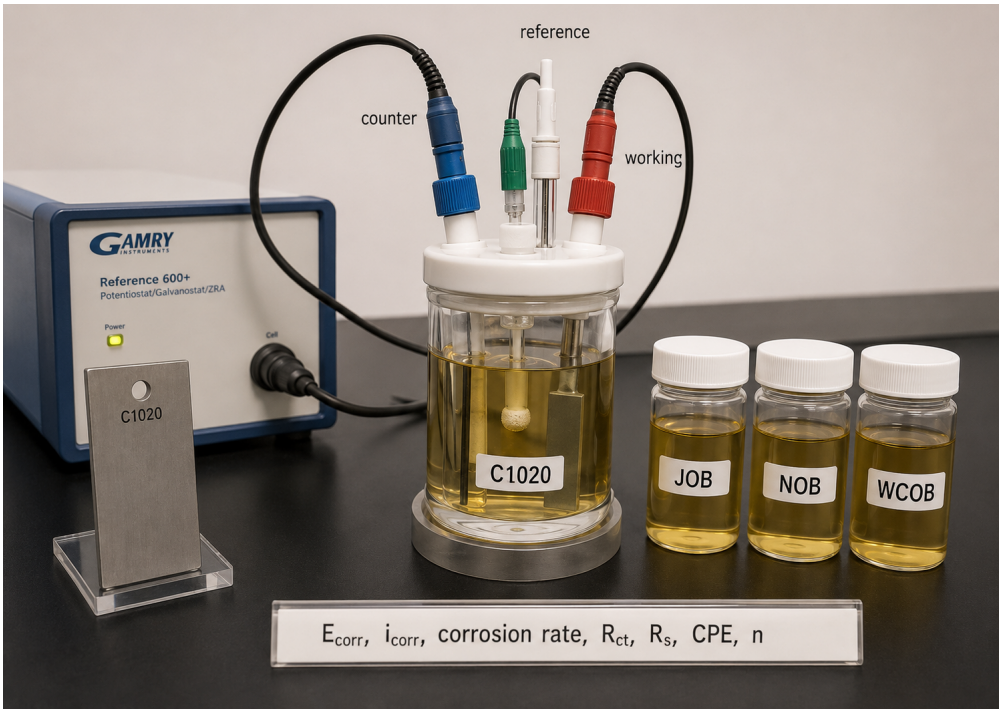

Figure 1: Electrochemical test cell.

This arrangement makes it clear why the study analyzes the fuel chemistry along with its interfacial effect. Biodiesel exists in the aqueous cell, while the corrosion ranking is defined based on the interface contacting the C1020 steel. Therefore,

the quantities such as i_{corr} and R_{ct} reflect the response of the steel in each test fluid and not just some bulk property of the fuel.

The molecular-reactivity block starts by differentiating between polyunsaturated esters and saturated and monounsaturated ones. For fatty-acid species i, which accounts for x_i percent of the fuel and has b_i number of double bonds, the polyunsaturated fraction is estimated using the following equation:

$$P_{\geq 2} = \sum_{i=1}^{m} x_i H(b_i - 2). \tag{1}$$

Here H is a Heaviside step function and is unity only if $b_i \geq 2$. This mathematical form reflects a clear chemical meaning. Methyl oleate cannot be considered equivalent to methyl linoleate or methyl linolenate. Oleates contribute to the iodine value; however, esters with two or more double bonds are expected to be more reactive due to their additional reactive unsaturation positions.

The quadratic unsaturation density, U_Q, is defined as follows:

$$U_Q = \sum_{i=1}^{m} x_i b_i^2. \tag{2}$$

As shown above, the squared value makes the effect of multiply unsaturated species stronger. This calculation does not aim to recreate the complex autoxidation kinetic modeling framework. The value of U_Q is used only for comparison, and helps to compare a mixture rich in oleic acids with another rich in multiple unsaturations. For the selected fuel group, the descriptor is highly important, because despite the relatively high iodine value of WCOB, it has very low $P_{\geq 2}$ and U_Q values.

The fuel side of activation, A_f, is defined as

$$A_f = A_v + F_{\mathrm{FFA}} + 10M_c, \tag{3}$$

where A_v is the acid value, F_{FFA} is the concentration of free fatty acids, and M_c is the moisture content. The multiplier for the last value allows assigning importance even to small amounts of moisture, which might promote the breakdown of esters, facilitate ion transport, and enable electrochemical reactions in an organic solvent. The activation descriptor is a screening parameter for these specific fuels. The goal is to see whether the acidity and water level confirm the molecule-based hazard identified previously.

Each harmful descriptor was normalized via min-max scaling,

$$\widehat{X}_j = \frac{X_j - X_{\min}}{X_{\max} - X_{\min}}. \tag{4}$$

Protective descriptors were multiplied by minus one. As for the charge-transfer resistance and the CPE exponent, the higher R_{ct} means the better protection, whereas the larger value of n is associated with a greater level of inhibition. Therefore, it was necessary to invert them so as not to contradict the general meaning of the score.

The molecular-reactivity load, L_M, was defined as

$$L_M = 100\left(0.35\widehat{U}_Q + 0.25\widehat{P}_{\geq 2} + 0.25\widehat{A}_f + 0.15\widehat{\eta}\right), \tag{5}$$

in which η refers to viscosity at 40 °C. Viscosity has been considered as a modifying variable but not as an initial cause of corrosion. A higher viscosity level in biodiesel may have influence on the properties such as wetting, product removal, residence time in the interface, and transfer of polar species. Higher weights were allocated to U_Q, $P_{\geq 2}$, and A_f, as these parameters quantify molecular oxidation pressure and activation due to acids and water.

The deficiency in interface shielding, D_I, was evaluated by

$$D_I = 100\left(0.28\widehat{i}_{\mathrm{corr}} + 0.25\widehat{CR} + 0.27(1 - \widehat{R}_{ct}) + 0.12\widehat{CPE} + 0.08(1 - \widehat{n})\right). \tag{6}$$

Combination of dissolution rates, corrosion-rate magnitude, charge-transfer shielding, and capacitive dispersion are used to interpret this equation. It could be said that a high surface current, high corrosion rate, low R_{ct}, high CPE, and low n result in a deficient and corrosive interface. The interface shielding block determines whether the electrochemistry of the surface matches the molecular chemistry of the fatty acid composition.

Finally, the MRIS index for risk assessment and the compatibility of the biodiesel and steel pair are given by

$$S_{\mathrm{MRIS}} = 0.45L_M + 0.55D_I, \qquad C_{\mathrm{BSC}} = 100 - S_{\mathrm{MRIS}}. \tag{7}$$

The interface block is assigned a slightly higher weight than the molecular block since compatibility depends on the measured response of the steel to the biodiesel composition. Molecular descriptors carry equal importance, as they determine the reasons behind the interface activation. High compatibility is indicated by scores near 100, while a low compatibility score implies the lowest risk in this set of three biodiesels. Therefore, the score is an index of C1020-biodiesel compatibility in the three cases.

3. Results and discussion

Figure 2 provides a comprehensive visual representation of the steel-biodiesel system prior to the description of each descriptor. The three fuels cannot be considered as a set of interchangeable biodiesels. JOB is characterized by the greatest level of polyunsaturation of the fuel and the highest level of steel response, NOB has an acidity and free-fatty-acids activating effect along with a medium response in the electrochemical analysis, and WCOB is an oleic fuel with the lowest corrosion current density and the highest charge-transfer resistance. In the case of this comparison (JOB > NOB > WCOB), the data presented in tables **??** and **??** is used to derive the severity of the corrosion phenomenon.

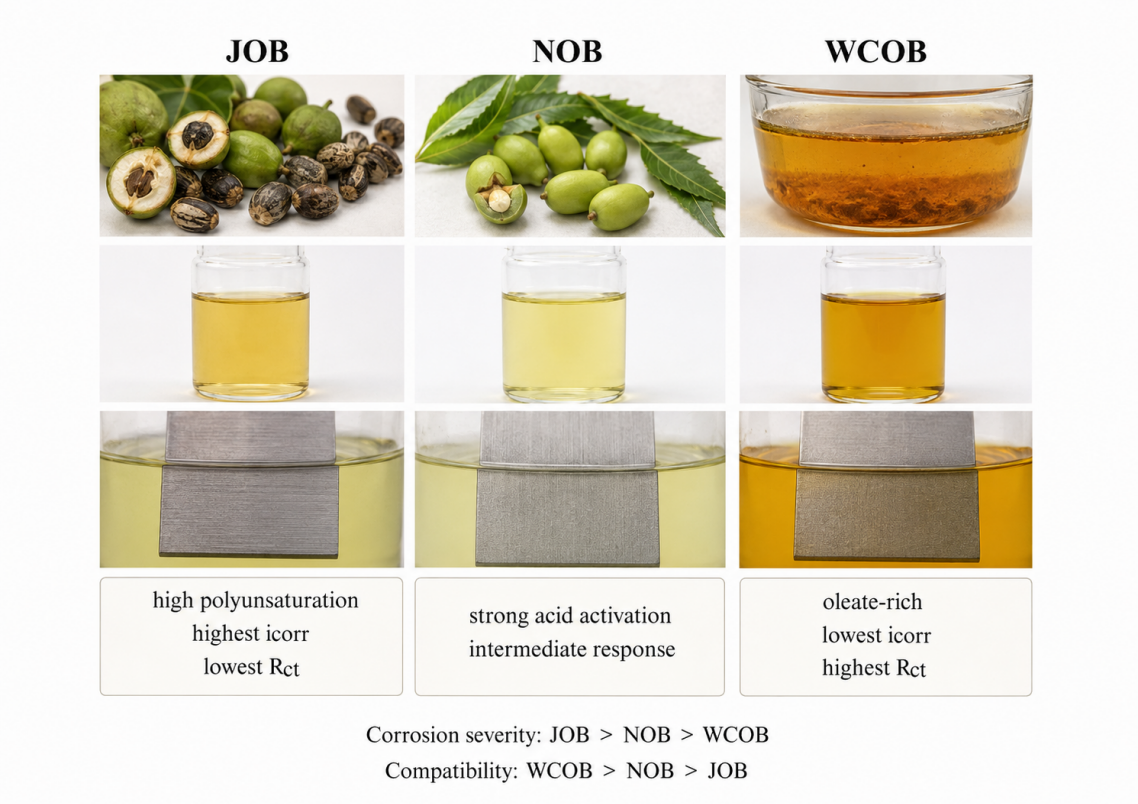

Figure 2: Steel-biodiesel compatibility overview.

Such an approach is helpful since all four key aspects of the process are included in the picture: source, fuel, metal contact, and outcome. According to Figure 2, JOB is the least favourable environment for C1020 due to the high polyunsaturation and the lowest values of i_{corr} and R_{ct}. NOB cannot be considered a visual and mechanistic analogue of JOB since its primary characteristic is the presence of acidic activation, not the polyunsaturated component. The chemical and electrochemical nature of WCOB is unique, as it has the lowest i_{corr} and the highest R_{ct}, as well as an oleic nature of the composition. Therefore, one of the fundamental conclusions that the paper makes based on its findings can be presented: compatibility is related to coupled fuel chemistry and charge transfer, not the name and polyunsaturative characteristics of the biodiesel.

The fatty-acid composition profile in Figure 3 provides a breakdown of saturated, monounsaturated, and polyunsaturated fuel components. For JOB, polyunsaturation is the dominant component, with C18:2 representing the highest proportion of unsaturated compounds, equal to 35.281%. In the case of NOB, there is a relatively high content of monounsaturated fraction C18:1 (37.4%) and a high polyunsaturated component (35.300%). WCOB stands out due to a very high level of C18:1 (90.21%) and a relatively low polyunsaturated fraction (0.420%).

These compositions in Figure 3 show the reason for why the term unsaturation needs to be split into two parts - monounsaturated and polyunsaturated - in the calculations of MRIS. Fuel with high content of C18:1 can possess high iodine value due to the large amount of double bonds, which, however, are spread evenly with respect to one double bond per each chain within a population rich in oleate. Fuel, on the other hand, enriched with C18:2 and other multivalent unsaturated molecules possesses higher number of oxidation sensitive positions in terms of molecule. It is the reason for why JOB but not WCOB represents the most reactive fuel according to MRIS calculations. Iodine value alone is therefore an incomplete structure indicator [21]. Fuel properties also depend on the detailed structure of the fatty-acid alkyl esters [11]. Fatty-acid composition influences several biodiesel properties relevant to stability and compatibility [12]. Oxidation-stability reviews support this distinction between total unsaturation and actual degradation behavior [8]. The visual interpretation is therefore aligned with the general understanding of how fatty-acid structure determines biodiesel oxidative stability [10].

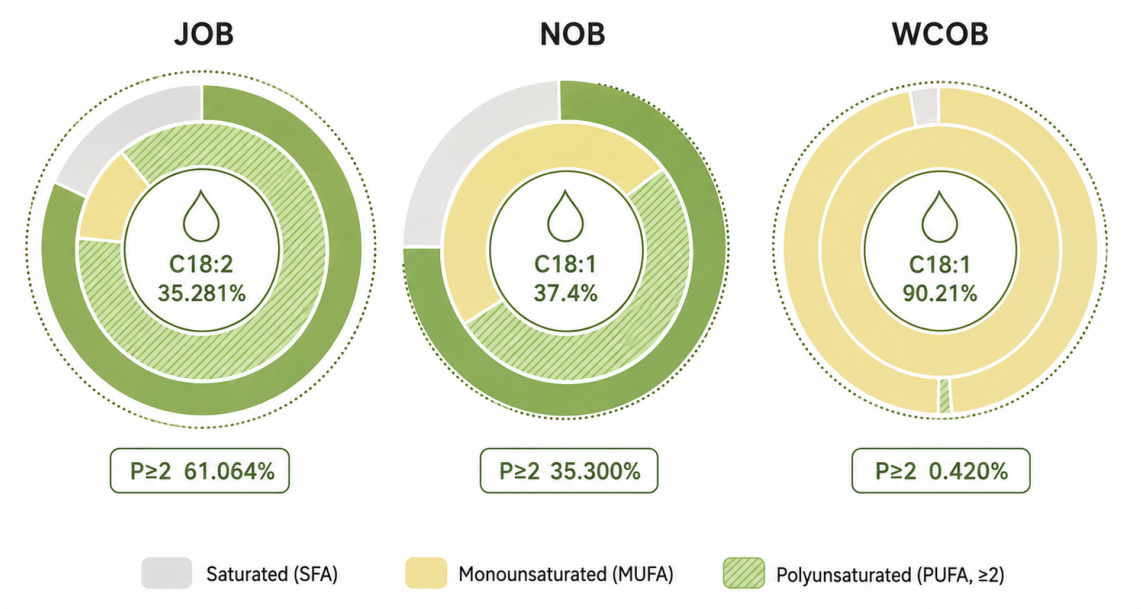

Figure 3: Fatty-acid composition profile.

The oxidative-burden map shown in Figure 4 validates this reasoning with quantitative interpretation. The horizontal axis shows the polyunsaturated fraction, the vertical one shows U_Q index, and size of the bubbles reflects the corresponding iodine value. While WCOB fuel carries the largest bubble with respect to iodine value but remains located at the edge of the map characterized by low-$P_{\geq 2}$ and low-U_Q indexes, JOB fuel possesses smaller bubble with respect to iodine value but occupies the position with highest oxidative burden, namely $P_{\geq 2} = 61.064\%$ and $U_Q = 325.777$. NOB fuel remains in between, namely at $P_{\geq 2} = 35.300\%$ and $U_Q = 201.400$.

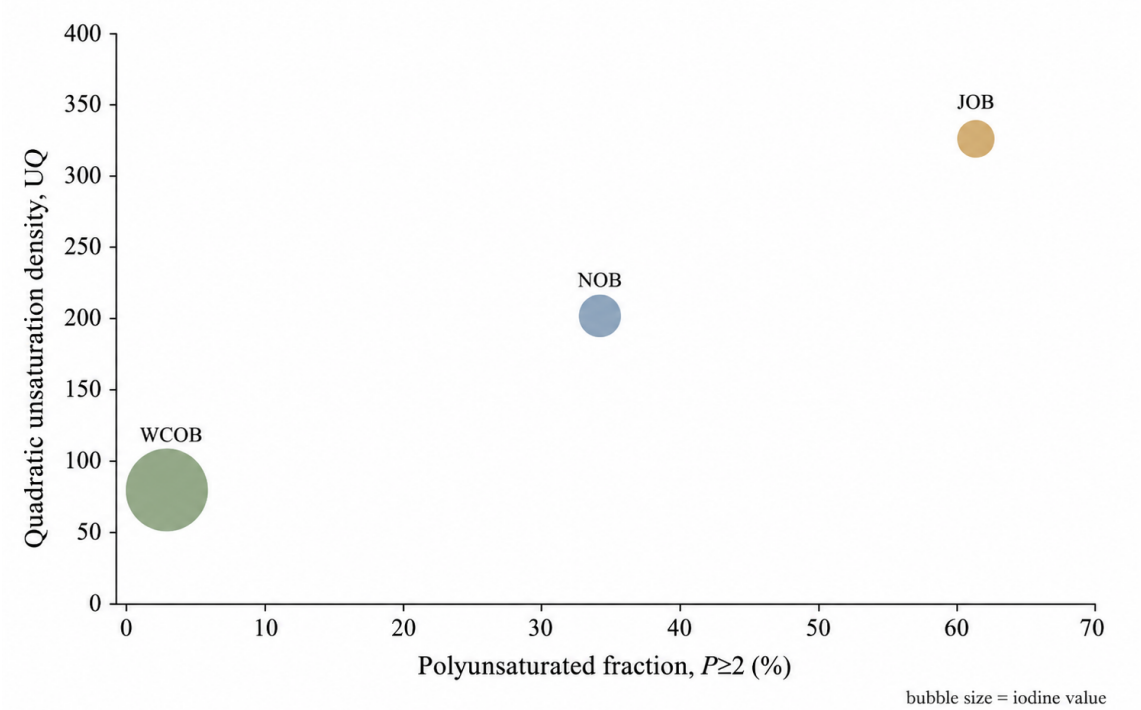

Figure 4: Oxidative burden map.

The placement of the bubbles on the oxidative burden map confirms the failure of simple iodine value compatibility rule. If iodine value was responsible for C1020 corrosion rate, the ranking would have been completely different from the results obtained experimentally since WCOB fuel has iodine value of 86.40 g I_2 per 100 g oil. On the other hand, JOB ranks as the worst fuel due to the presence of more polyunsaturated fatty acids in it, while WCOB fuel comprises primarily mono-unsaturated fatty acids. The significant gap between JOB and WCOB fuel both with respect to polyunsaturated fraction and U_Q index validates the choice of these molecular parameters together with conventional fuel indices as the basis for compatibility assessment.

The activation field in Figure 5 locates the fuels relative to their acid values, free fatty acid, and moisture, with

the corresponding A_f values presented as markers. NOB exhibits the highest contribution to acid/free-fatty-acid and, consequently, the maximum activation factor, $A_f = 1.704$. JOB possesses lower activation factor, $A_f = 1.397$, but the highest moisture content and viscosity, respectively, among the other two fuels in Table 1. WCOB belongs to the low-activation range of the field with $A_f = 0.597$, due to the fuel's low acid value and low moisture content.

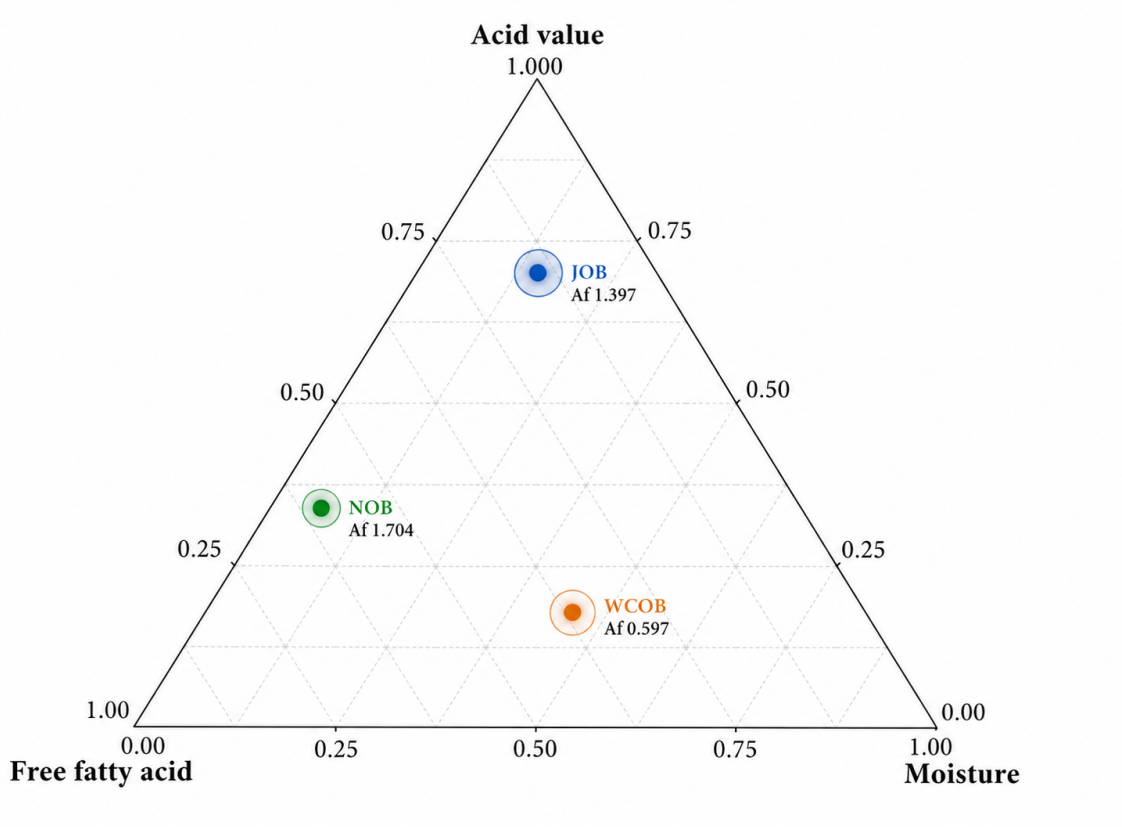

Figure 5: Physicochemical activation field.

In Figure 5, one can clearly see the reason behind the fact that the corrosion ranking cannot be defined based solely on the acid value. NOB demonstrates greater chemical activation by means of the A_f indicator than JOB, whereas JOB exhibits higher current density and corrosion rate. The explanation is that chemical activation alone constitutes only one aspect of the corrosion mechanism. Molecular oxidation pressure and interfacial resistance should be considered alongside it. In the case of NOB, the acid value and free fatty acid should be controlled; however, the more severe situation relates to JOB, where higher polyunsaturation goes along with much smaller charge transfer resistance. WCOB represents the favourable position as indicated by both the activation field and impedance results.

The polarization portrait in Figure 6 shows correlation between $E_{\text{corr}}$and log-transformed i_{corr}, with marker size indicating the corrosion rate. For JOB, one observes high current density, i.e., corrosion rate, with E_{corr}=-586 mV, i_{corr}=16.23 μA cm^{-2}, and corrosion rate being 103 mpy. NOB features more negative corrosion potential and lower current density, i_{corr}=11.47 μA cm^{-2}; the same applies to WCOB, which exhibits the lowest current density with E_{corr}=-594 mV and i_{corr}=5.74 μA cm^{-2}.

As can be seen from the polarization plot shown in Figure 6, corrosion potential is inadequate as a measure of severity for the biodiesel media considered. The WCOB biodiesel medium exhibits the lowest corrosion potential, however, it is the least severe medium by current and corrosion rate. A more important indicator is i_{corr}which follows the same order of severity as the corrosion rates in Table 2. High JOB value is associated with fast dissolution, whereas WCOB corresponds to the minimal rate of material loss among the tested biodiesel mediums. Mixed-potential theory explains why corrosion potential alone cannot represent metal-loss kinetics [26]. Corrosion-science interpretation likewise requires the current response to be considered with the surface process [25].

In addition to charge transfer resistance, impedance state map presented in Figure 7 involves two more parameters, CPE exponent and CPE magnitude. JOB is placed in low-R_{ct}, low-n area and has the largest marker since it possesses the highest CPE magnitude. In turn, WCOB is located farthest from the JOB position, namely in an area characterized by $R_{\text{ct}} = 601$ Ω cm^2, $n = 0.94$ and the lowest CPE magnitude. NOB, finally, falls midway, having $R_{\text{ct}} = 270$ Ω cm^2 and $n = 0.89$.

Based on the analysis of impedance state map in Figure 7, one can conclude about the surface condition corresponding to the kinetic sequence JOB > NOB > WCOB. Low R_{ct} is indicative of poor charge transfer resistance, whereas the lower value of the CPE exponent and higher CPE magnitude point either to higher capacitive dispersion or greater heterogeneity of the surface layer. Therefore, JOB corresponds to the surface that provides the most favorable interface for corrosion,

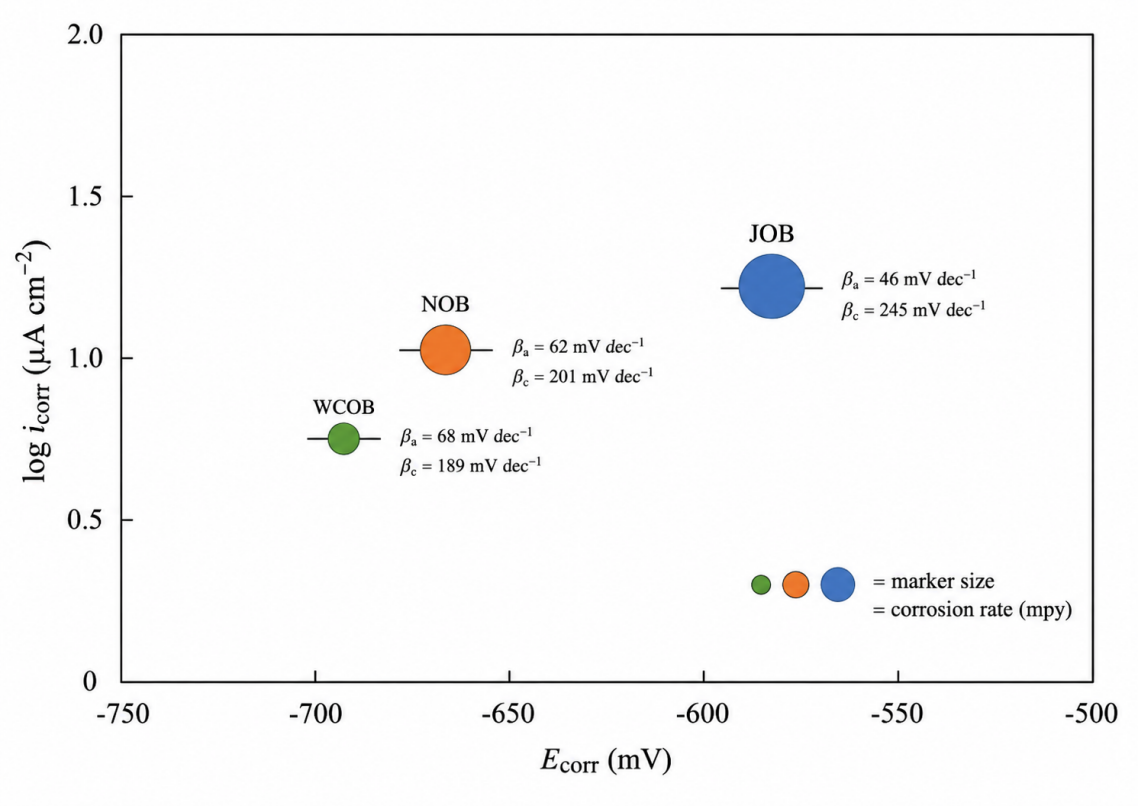

Figure 6: Polarization descriptor portrait.

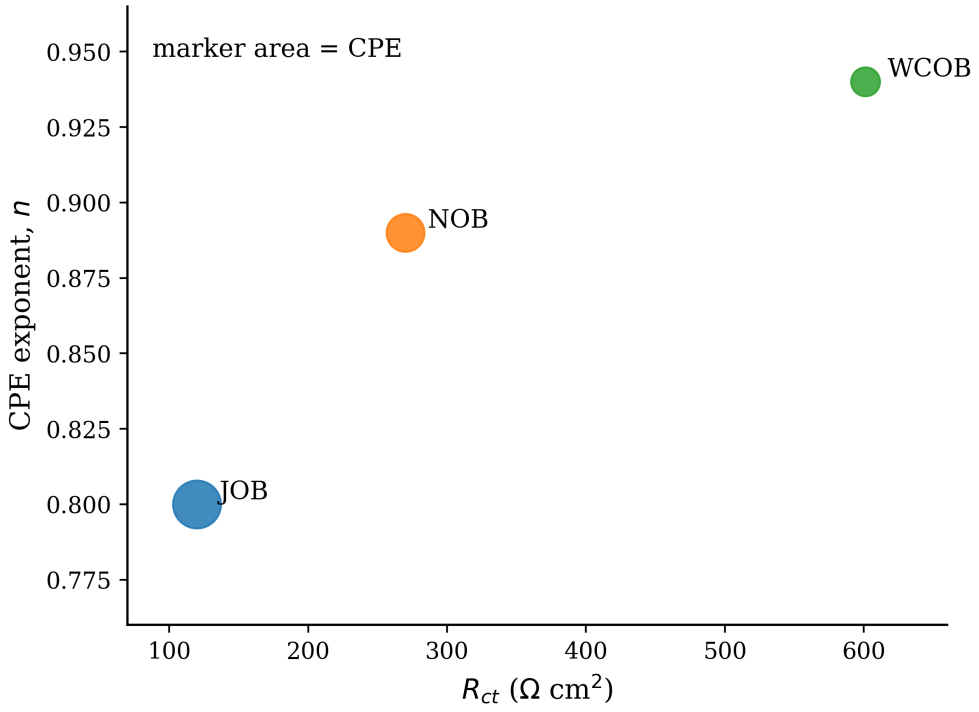

Figure 7: Impedance state map.

whereas WCOB, with high R_{ct} and more ideal capacitance, is the most compatible biodiesel medium. EIS is a useful method for distinguishing charge-transfer resistance and coating or film behavior [23]. The interpretation of faradaic impedance supports this reading of interfacial resistance [22]. Modern EIS analysis further connects constant-phase behavior with heterogeneous interfaces [24]. Impedance data therefore provide the best evidence in favor of WCOB > NOB > JOB.

The ratio comparison presented in Figure 8 turns the quantities presented in Table 3 into the severity representation. JOB has the highest ratio values: $\eta/R_{ct} = 0.0583$, $i_{corr}/R_{ct} = 0.1353$, and $CR/R_{ct} = 0.8583$. The ratios for NOB are smaller compared to those for the other oils, despite its highest value of A_f, while WCOB has the smallest ratios on all tracks. This is due to the logarithmic axis used, where the separation of JOB from WCOB is clearly visible.

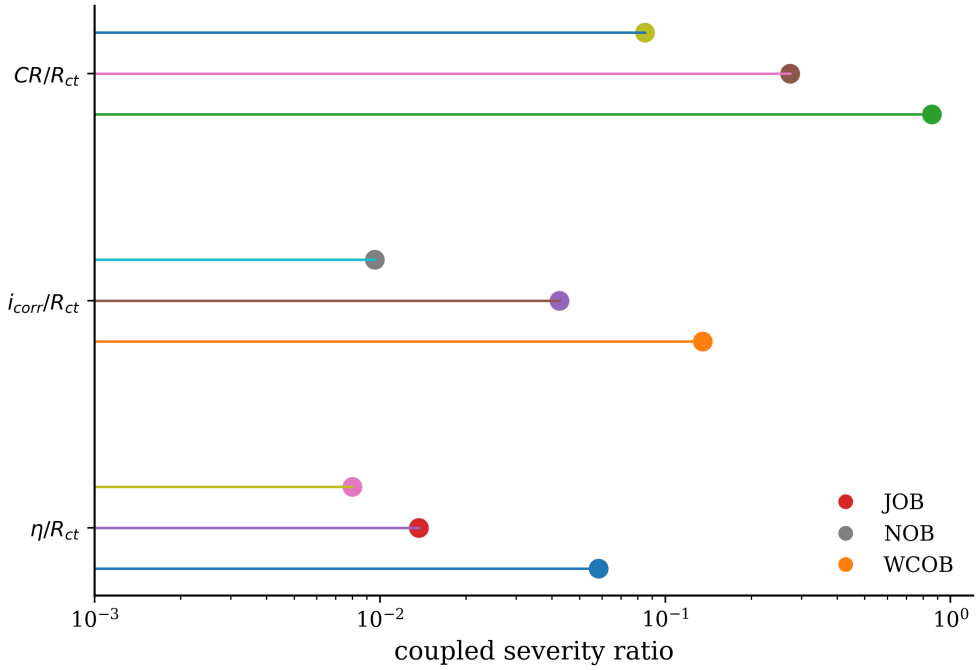

Figure 8: Coupled severity ratios.

These ratios are essential since they reflect both transport or dissolution severity and interface resistance. High η/R_{ct} for JOB indicates a contacting state where polar decomposition products form close to the less well-shielded steel surface. The current-to-resistance and corrosion rate-to-resistance ratios indicate that the high activity of the dissolution process is combined with low charge transfer resistance. NOB is still relevant from a chemical point of view; however, the increase in R_{ct} leads to the decrease of the severity ratios. WCOB yields the lowest ratio values, due to high resistance to charge transfer at its interface.

The panels of cross relations in Figure 9 illustrate two competing explanations of the order of current densities. In the panel for U_Q, there is an increasing relationship for WCOB, NOB, and JOB that coincides with the increasing order of corrosion currents. However, in the A_f panel, NOB possesses the largest value of the activation factor; on the other hand, JOB exhibits the largest value of i_{corr}. The two panels therefore separate polyunsaturated oxidative pressure from acid-water activation.

Comparison presented in Figure 9 provides an unequivocal response to the main mechanistic question posed. Corrosion current direction is better aligned with the polyunsaturation-adjusted molecule structure rather than with isolated activation parameter. It should not be taken for a lack of importance of acidity since acid activation must act via surface that allows charge transfer. NOB demonstrates significant acid and free-fatty acid activation, yet it does not satisfy the requirement of both U_Q being high and R_{ct} being low, hence the fact that JOB is a most corrosive system. WCOB still maintains low currents due to insufficiently developed activation parameter and low molecular burden parameters against high interfacial resistance.

Contribution profile presented in Figure 10 explains the normalized MRIS score formation. JOB gets considerable contributions from such factors as U_Q, $P_{\geq 2}$, i_{corr}, corrosion rate and inverse resistance. NOB shows significant activation contributions as well as low electrochemical and polyunsaturation contributions compared to JOB. WCOB gets insignificant overall contributions due to both low $P_{\geq 2}$ and A_f parameters and extremely high R_{ct} value.

The stacked bar representation of Figure 10 makes the calculated index transparent. The score is calculated not according to an invisible and univariable rule. JOB is a high-risk material since the index value of both electrochemical and molecular components is high. NOB is an intermediate one, as acid/free-fatty-acid activation plays an essential role, yet is not

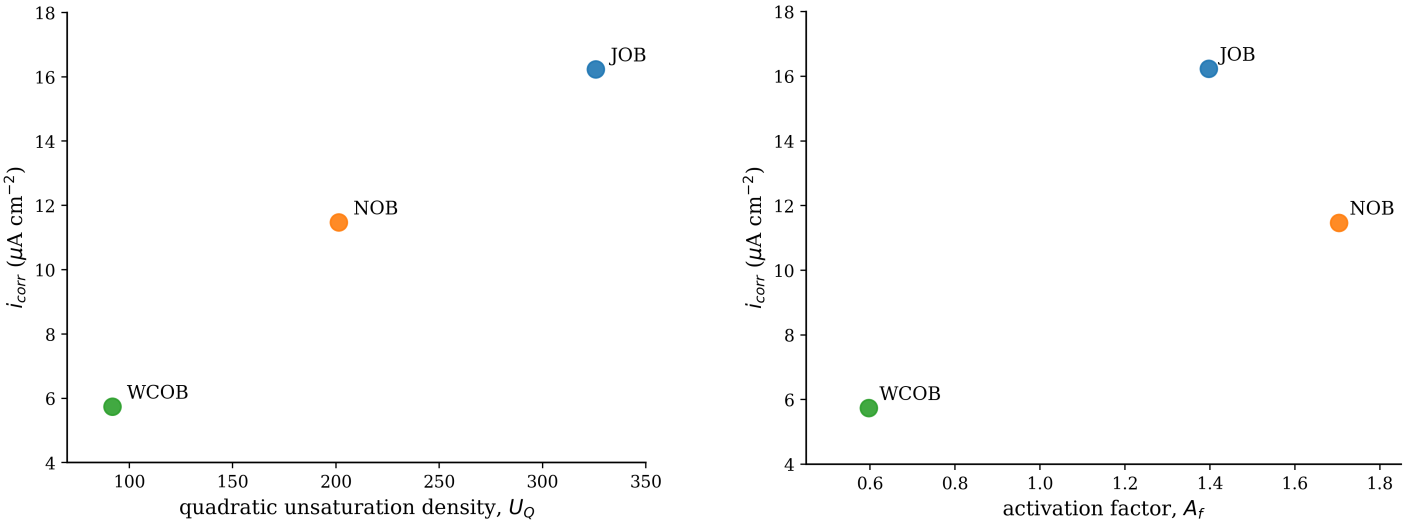

(a) U_Q and current.

(b) A_f and current.

Figure 9: Composition-activation links to current.

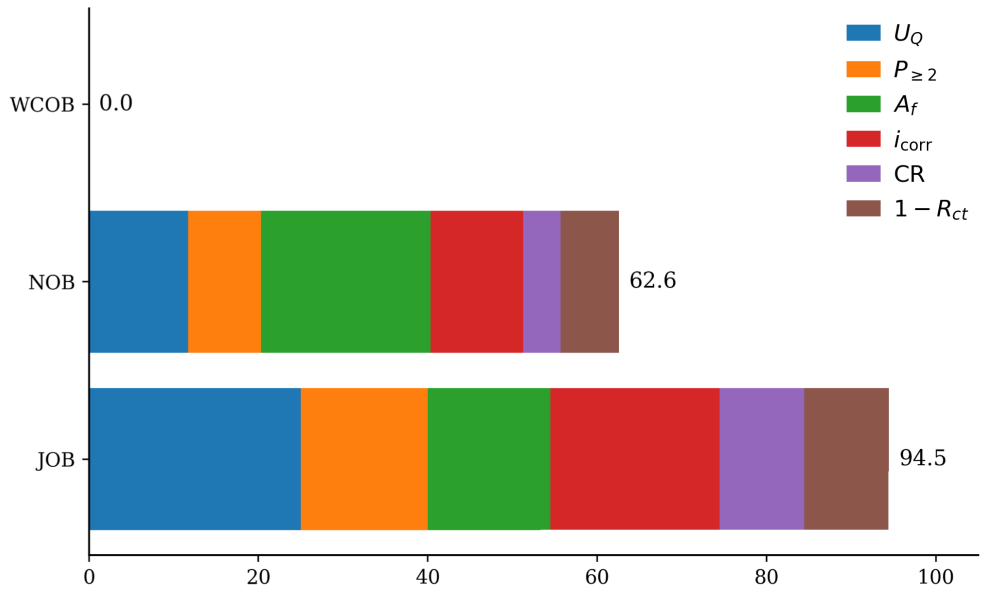

Figure 10: Susceptibility contribution profile.

coupled with maximum polyunsaturation or minimum charge transfer shielding. In its turn, WCOB can be considered as a favourable material since the positive effects of both protective interface term and low polyunsaturation burden coincide. Such decomposition helps to understand the role that each type of material susceptibility plays for engineering decision-making. Thus, the oxidation process needs to be controlled in JOB, while acid/moisture level is crucial in the case of NOB. Finally, it is necessary to make sure of good quality in WCOB.

The compatibility ladder of Figure 11 is used to convert MRIS into the positive compatibility number C_{BSC}. WCOB is assigned to the favourable end of the ladder, $C_{\mathrm{BSC}} = 97.78$, while NOB still stays in the middle, $C_{\mathrm{BSC}} = 45.90$. The placement of JOB is near the unfavourable end of the ladder, $C_{\mathrm{BSC}} = 3.12$.

The ranking in Figure 11 should be viewed as the comparison for C1020 steel among the three tested fuels. WCOB cannot be claimed non-corrosive in any case, since the biodiesel produced from the waste might differ depending on the type of feedstock used, frying conditions, water content, and existing oxidation levels. NOB cannot be considered safe, since its corrosion rate is as high as 74 mpy and the acid and free fatty acid-based activation is the highest in this group. JOB is the worst of all because both chemical and electrochemical parameters support the same trend. Thus, the relative significance order remains unambiguous: JOB > NOB > WCOB in terms of potential corrosion, and WCOB > NOB > JOB regarding compatibility of C1020 steel with the tested fuels.

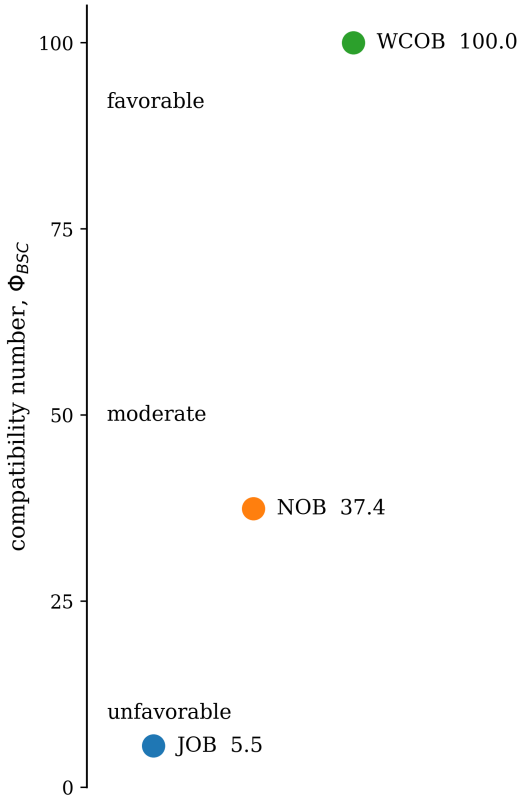

Figure 11: Compatibility ladder.

The listed parameters in Table 3 characterize the mechanism of the ranking order presented in Figure 11. JOB features the highest viscosity/resistance, current/resistance, and corrosion rate/resistance ratios. Thus, this fuel creates favorable conditions for interaction with metal by providing weak electrochemical barriers. Although NOB provides the highest A_f, its ratio values are considerably lower compared to the values reported for JOB due to higher resistivity. Finally, WCOB provides the smallest values for all of the ratios, which means the lowest resistance to charge transfer at steel interfaces among the tested fuels.

Three different routes of corrosion appear based on entries in Table 3. JOB is primarily governed by a coupled route: polyunsaturation, high viscosity, high current density, high corrosion rate, and low R_{ct}. NOB is governed by an acid/free-fatty-acid activation route and an intermediate interface response. WCOB is driven by oleate-enriched activation and charge-transfer shielding. Consequently, Table 3 shows that NOB is not necessarily the most corrosive fuel despite its high acid/free-fatty-acid value. Severity of corrosion depends on the combined action of activation chemistry, molecular oxidizing pressure, and interface resistance.

Combining the results of the chemical and electrochemical analyses presented in Figures 2–11 gives the MRIS ranking result presented in Table 4. The highest risk score belongs to JOB (96.88) followed by a lowest compatibility number (3.12). The intermediate risk and compatibility numbers belong to NOB (risk score 54.10; compatibility number 45.90). The

Table 3: Derived MRIS descriptors.

Descriptor	JOB	NOB	WCOB
$A_f = A_v + F_{\mathrm{FFA}} + 10M_c$	1.397	1.704	0.597
η/R_{ct}	0.0583	0.0137	0.0080
$i_{\mathrm{corr}}/R_{\mathrm{ct}}$	0.1353	0.0425	0.0096
CR/R_{ct}	0.8583	0.2741	0.0849
Molecular load, L_M	93.07	55.77	4.93
Interface deficit, D_I	100.00	52.74	0.00

smallest risk score is assigned to WCOB (2.22) whereas the highest compatibility number belongs to WCOB (97.78). Thus, the order of severity is JOB > NOB > WCOB.

Table 4: MRIS compatibility classification.

Biodiesel	S_{MRIS}	C_{BSC}	Compatibility interpretation
JOB	96.88	3.12	Severe risk from high polyunsaturated molecular load combined with weak charge-transfer shielding.
NOB	54.10	45.90	Managed/intermediate risk from strong acid/free-fatty-acid activation moderated by intermediate resistance.
WCOB	2.22	97.78	Favourable condition from oleate-rich composition, low activation, and strongest charge-transfer resistance.

The classification provided in Table 4 is decision-oriented. The statement that WCOB is non-corrosive or that NOB is ignorable should be avoided. The corrosion rate for NOB is 74 mpy and that of WCOB is 51 mpy under the evaluated conditions. The compatibility number should be considered relative in the studied sample set. However, what its value signifies is that the underlying controlling mechanism becomes known. JOB needs both oxidation and surface protection measures. NOB requires control on both acid values and free fatty acid concentrations. WCOB requires quality verification and monitoring as waste-based biodiesels can have significant variance regarding the feedstock sources and thermal history.

The mechanistic route of the first biodiesel sample (JOB) is the most aggressive due to the combination of aggressive product formation and electrochemical allowance. An abundant population of polyunsaturated esters leads to the accumulation of peroxides and acidic oxidative by-products during storage, especially with oxygen and water presence, as well as exposure to high temperatures and metals. JOB exhibits a relatively high moisture content and high viscosity of all fuels. Both factors increase polar products persistence on the steel surface and reduce their clearance rate. After surface activation, the very low R_{ct}value signifies that there are no sufficient barriers to charge transfer. As a consequence, a considerable corrosion current density and corrosion rate result from this pathway. Thus, this mechanistic explanation is the rationale behind the strictest corrosion management strategy for JOB in the C1020 steel service environment.

On the contrary, the second biodiesel sample (NOB) exhibits a high acid factor, which results from acid and free fatty acid values rather than a dominant presence of a strongly unsaturated compound. Therefore, the management strategy of the first biodiesel sample can be adapted but with additional focus on purification and reduction of free fatty acids, along with storage in dry conditions and frequent acid-number testing. The intermediate MRIS classification does not signify a negligible impact on corrosion. A corrosion rate of 74 mpy is substantial and the high activation factor implies that an increased amount of water or oxidation may tip the balance in the wrong direction. The rationale behind this sample lagging behind JOB is that the interface resistance and polyunsaturated pressure values of NOB are superior. This is precisely the kind of mechanistic discrimination that would not be expressed in a single corrosion rate or fuel property table.

The mechanistic route for WCOB is advantageous in the selected set due to synergy between oleate-rich composition and interface resistance. Contrary to the popular opinion, high iodine value means a high concentration of monounsaturated compounds. Oleate has just one double bond and thus has a lower unsaturation value. All indicators of a minimal corrosion risk (low acid value, moisture content, small CPE magnitude, and high n and R_{ct} values) contribute to the lowest corrosion rate observed in the tested set. Waste-cooking-oil biodiesel can have variance regarding quality due to improper feedstock collection and over-frying, which can increase acidity, polymerization, moisture, and metallic content. However, among the three tested fuels, WCOB is the most compatible with C1020 carbon steel.

These findings have consequences for specification-based practice. The sequence of flash points does not correspond to

the sequence of iodine values and the sequence of corrosivities. WCOB has the largest flash point and iodine value and the best compatibility response. JOB has the smallest flash point but a very strong corrosion response, although it is not solely governed by flash point. NOB has the largest acid/free fatty acid load but not the largest corrosion current. All these examples confirm the need to use a multi-descriptor decision making process in compatibility. ASTM-related biodiesel quality testing provides important fuel-control boundaries [19]. EN 14214 also defines requirements for fatty-acid methyl ester fuels [20]. Automotive-system compatibility reviews show that these quality boundaries do not remove the need for interface-specific materials assessment [6]. Carbon steel compatibility assessment must therefore include an extra layer of interpretation for different feedstocks.

The MRIS score is a relative three-fuel measure rather than a natural law. The min-max normalization applies exclusively to JOB, NOB, and WCOB, and hence the class labels used for each fuel are comparative. The development of thresholds for universal compatibility evaluation would require additional fuels, replicated experiments, extended immersion, altered temperatures, antioxidants, controlled water addition, and variation in oxygen level. The utility of the score lies in the fact that the sense of each variable is physical. The increased values of U_Q, $P_{\geq 2}$, A_f, viscosity, i_{corr}, corrosion rate, and CPE magnitude imply greater danger, while the increased values of R_{ct} and n mean reduced risks. The calculation of the MRIS is easily verifiable and extensible to any other group of fuels.

This study also shows some interesting trends when comparing to previous work. Material compatibility research has emphasized that biodiesel corrosivity is affected by hygroscopicity, oxidizability, and the formation of acidic and polar degradation products [16]. Automotive-material reviews similarly identify corrosion and compatibility as important issues in biodiesel service [28]. Biodiesel-system compatibility studies further stress that fuel chemistry and component material must be considered together [6]. The current experimental results refine this general notion through the specific example of three neat biodiesels acting differently on one and the same carbon steel sample. For example, JOB corrodes the metal at least 2.83 times faster, and WCOB provides around 5 times larger resistance. The significant differences would not emerge if only the generalization that the three fuels are biodiesels was stated. Therefore, fuel compatibility is both feedstock and interface dependent.

Future studies could involve connecting MRIS ranking with additional surface and fuel analysis. It will include measurements of mass loss, optical profilometry, SEM/EDS, Raman spectroscopy, FTIR, XPS, soluble metal content, peroxide value, post-immersion acid value, and water content. Long-term exposure is essential since biodiesel can degrade during storage. At initial stages, the surfaces might form coatings which later separate, break, or transform into a different substance. The galvanic effect in presence of copper-alloyed metals and microbial contamination should also be considered in real fuel storage and delivery systems.

4. Conclusion

C1020 carbon-steel compatibility with jatropha, neem, and WCO biodiesels does not correlate with the total amount of unsaturation. Despite having the highest iodine value, WCOB is also the most compatible fuel among the tested samples. The reason for this is that WCOB has high oleic content, lowest polyunsaturates' amount 0.420%, lowest acid-water activation factor 0.597, lowest corrosion current density 5.74 μA cm^{-2}, lowest corrosion rate 51 mpy, and highest charge-transfer resistance 601 Ω cm^2.

JOB is the most challenging system due to the combination of high reactivity and weak interaction at the interface. Among the investigated fuels, it has the highest polyunsaturated fraction 61.064%, quadratic unsaturation density 325.777, corrosion current density 16.23 μA cm^{-2}, corrosion rate 103 mpy, and lowest charge-transfer resistance 120 Ω cm^2. All these factors indicate that the steel surface comes under attack both by strong oxidative degradation products and has low kinetic barriers to charge transfer. As a result, the estimated MRIS value of 96.88 marks JOB as the fuel which needs the tightest corrosion management procedures for C1020 steel.

NOB has an intermediate position due to a high chemical activation and comparatively weak molecule and electrochemical burden. Having the highest activation factor 1.704 proves that acid value and free fatty acids should be carefully controlled, but at the same time, relatively high charge-transfer resistance and low polyunsaturates' density make NOB a less harmful fuel than JOB. With the MRIS risk score of 54.10, NOB is assigned to the group of managed compatibility.

Thus, the final ranking of biodiesel fuels by compatibility with C1020 steel in terms of corrosion resistance is WCOB > NOB > JOB, and according to corrosion risk, the sequence is JOB > NOB > WCOB. This demonstrates that C1020 steel compatibility depends on a combined effect of the presence of polyunsaturated esters, acid-water activation, and charge-transfer shielding. Iodine value still remains a helpful characteristic for assessing overall fuel chemistry, but it can be misleading when the amounts of oleic acids and polyunsaturates differ substantially.

MRIS number is internally normalized for three biodiesel fuels and a specific steel grade. Further investigation on

different feedstocks, blend ratios, antioxidant treatments, water content, temperature history, storage times, and repeated electrochemical testing will be required to set thresholds for more generalized applications. Surface chemical analysis and post exposure analysis of test fuels may be used to verify the predicted risk classes by matching them with the morphological characteristics of corrosion, released dissolved metals, oxides/organics produced, and biodiesel degradation stage. In the scope of the evaluated biodiesels, the practical answer to compatibility is WCOB being the best matching fuel, NOB needing acid and moisture management, and JOB requiring complete control of oxidative processes and interface protection.

Conflict of interest

The author declares no conflict of interest.

References

[1] Marchetti, J. M., Miguel, V. U., & Errazu, A. F. (2007). Possible methods for biodiesel production. Renewable and sustainable energy reviews, 11(6), 1300-1311.
[2] Moser, B. R. (2009). Biodiesel production, properties, and feedstocks. In Vitro Cellular & Developmental Biology-Plant, 45(3), 229-266.
[3] Hoekman, S. K., Broch, A., Robbins, C., Ceniceros, E., & Natarajan, M. (2012). Review of biodiesel composition, properties, and specifications. Renewable and sustainable energy reviews, 16(1), 143-169.
[4] Atabani, A. E., Silitonga, A. S., Ong, H. C., Mahlia, T. M. I., Masjuki, H. H., Badruddin, I. A., & Fayaz, H. (2013). Non-edible vegetable oils: a critical evaluation of oil extraction, fatty acid compositions, biodiesel production, characteristics, engine performance and emissions production. Renewable and sustainable energy reviews, 18, 211-245.
[5] Shahid, E. M., & Jamal, Y. (2011). Production of biodiesel: a technical review. Renewable and Sustainable Energy Reviews, 15(9), 4732-4745.
[6] Sorate, K. A., & Bhale, P. V. (2015). Biodiesel properties and automotive system compatibility issues. Renewable and Sustainable Energy Reviews, 41, 777-798.
[7] Jain, S., & Sharma, M. P. (2010). Stability of biodiesel and its blends: a review. Renewable and sustainable energy reviews, 14(2), 667-678.
[8] Pullen, J., & Saeed, K. (2012). An overview of biodiesel oxidation stability. Renewable and Sustainable Energy Reviews, 16(8), 5924-5950.
[9] Atadashi, I. M., Aroua, M. K., Aziz, A. A., & Sulaiman, N. M. N. (2012). The effects of water on biodiesel production and refining technologies: A review. Renewable and sustainable energy reviews, 16(5), 3456-3470.
[10] Yaakob, Z., Narayanan, B. N., & Padikkaparambil, S. (2014). A review on the oxidation stability of biodiesel. Renewable and Sustainable Energy Reviews, 35, 136-153.
[11] Knothe, G. "Dependence of biodiesel fuel properties on the structure of fatty acid alkyl esters." *Fuel Processing Technology* **86**.10 (2005): 1059–1070.
[12] Ramos, M. J., Fernández, C. M., Casas, A., Rodríguez, L., & Pérez, Á. (2009). Influence of fatty acid composition of raw materials on biodiesel properties. Bioresource technology, 100(1), 261-268.
[13] Yang, Z., Hollebone, B. P., Wang, Z., Yang, C., & Landriault, M. (2013). Factors affecting oxidation stability of commercially available biodiesel products. Fuel processing technology, 106, 366-375.
[14] Kaul, S., Saxena, R. C., Kumar, A., Negi, M. S., Bhatnagar, A. K., Goyal, H. B., & Gupta, A. K. (2007). Corrosion behavior of biodiesel from seed oils of Indian origin on diesel engine parts. Fuel processing technology, 88(3), 303-307.
[15] Maru, M. M., Lucchese, M. M., Legnani, C., Quirino, W. G., Balbo, A., Aranha, I. B., ... & Achete, C. A. (2009). Biodiesel compatibility with carbon steel and HDPE parts. Fuel Processing Technology, 90(9), 1175-1182.
[16] Fazal, M. A., Haseeb, A. S. M. A., & Masjuki, H. H. (2011). Biodiesel feasibility study: an evaluation of material compatibility; performance; emission and engine durability. Renewable and sustainable energy reviews, 15(2), 1314-1324.
[17] Hu, E., Xu, Y., Hu, X., Pan, L., & Jiang, S. (2012). Corrosion behaviors of metals in biodiesel from rapeseed oil and methanol. Renewable energy, 37(1), 371-378.
[18] Jin, D., Zhou, X., Wu, P., Jiang, L., & Ge, H. (2015). Corrosion behavior of ASTM 1045 mild steel in palm biodiesel. Renewable Energy, 81, 457-463.
[19] Christensen, E. D., & McCormick, R. L. (2023). Water contamination impacts on biodiesel antioxidants and storage stability. Energy & Fuels, 37(7), 5179-5188.
[20] EN, B. (2019). 14214: 2012+ A2: 2019: Liquid Petroleum Products, Fatty Acid Methyl Esters (FAME) for Use in Diesel Engines and Heating Applications, Requirements and Test Methods. The British Standards Institution.
[21] Knothe, G. (2002). Structure indices in FA chemistry. How relevant is the iodine value?. Journal of the American Oil Chemists' Society, 79(9), 847-854.
[22] Lasia, A. (2013). Impedance of the faradaic reactions in the presence of mass transfer. In Electrochemical Impedance Spectroscopy and its Applications (pp. 85-125). New York, NY: Springer New York.
[23] Mansfeld, F. (1990). Electrochemical impedance spectroscopy (EIS) as a new tool for investigating methods of corrosion protection. Electrochimica Acta, 35(10), 1533-1544.
[24] Orazem, M. E., & Tribollet, B. (2008). Electrochemical impedance spectroscopy. New Jersey, 1(906), 383-389.
[25] McCafferty, E. (2010). Introduction to corrosion science. Springer Science & Business Media.
[26] Bard, A. J., Faulkner, L. R., & White, H. S. (2022). Electrochemical methods: fundamentals and applications. John Wiley & Sons.
[27] Adama, K. K., Onyeachu, I. B., Modebe, L. U., Chukwuike, V. I., Oghuma, P. O., & Akhabue, C. E. (2024). Comparative evaluation of corrosion behaviour of carbon steel (C1020) in different biodiesels: synthesis, characterization and electrochemical investigations. Results in Engineering, 21, 101695.
[28] Haseeb, A. S. M. A., Fazal, M. A., Jahirul, M. I., & Masjuki, H. H. (2011). Compatibility of automotive materials in biodiesel: A review. Fuel, 90(3), 922-931.